Appendix G

Summary of Survival Methods

Draft summary of methods used to simulate travel time, survival, and routing of juvenile Chinook salmon for the California WaterFix effects analysis.

R. Perry, USGS, Western Fisheries Research Center
19 December 2016

Here I provide a brief overview of the methods used to produce the draft results presented to the Independent Peer Review Panel's review for Phase 2B of the California Water Fix consultation. In summary, we combined equations from statistical models that estimate the relationship of Sacramento River inflows (measured at Freeport) on reach-specific travel time, survival, and routing of acoustic-tagged juvenile late-fall Chinook salmon. Given these equations, we simulated daily cohorts of juvenile Chinook salmon migrating through the Delta under the CalSim simulations of the Proposed Action (PA) and No Action Alternative (NAA). We also included daily Delta Cross Channel gate operations from the DSM2 simulations of PA and NAA.

Survival and Travel Time

Fitted models from a joint statistical analysis of travel time and survival in eight discrete reaches of the Delta (Figure 1, Perry et al. in prep.) was used for the assessing travel time and survival under the PA and NAA scenarios. The data for the analysis consisted of 2,170 acoustic-tagged late-fall Chinook salmon released during a five-year period (2007-2011) over a wide range of Sacramento River inflows (6,800 – 77,000 ft^3/s at Freeport). This analysis was based on acoustic telemetry data from several published studies where details of each study can be found (Perry et al. 2010, 2013; Michel et al. 2015).

Although a number of studies have identified a relationship between Delta inflows and survival at the Delta-wide scale, the goal of the Perry et al. (in prep.) analysis was quantify how the flow-survival relationship varies spatially among different regions of the Delta. To quantify the reach-specific relation between river inflows and survival, the analysis used time-varying individual covariates where an individual's covariate value was defined as the flow of the Sacramento River at Freeport on the day that *i*th fish entered the *m*th reach. Owing to missing covariate values for undetected fish, the analysis implemented the multistate mark-recapture model of Perry et al. (2010) using a complete data likelihood approach in a Bayesian framework (King et al. 2010). To cope with missing covariate values, the analysis jointly modeled both reach-specific travel times and survival. Estimated parameters of a log-normal travel time distribution for each reach were used to impute travel times of undetected fish, which in turn, allowed missing covariate values to be defined based on the imputed arrival time in a given reach. Markov Chain Monte Carlo techniques were used to integrate over the missing covariate values by drawing missing travel times on each iteration of the Markov chain.

Reach-specific survival and median travel time were modeled as functions of river inflow and DCC gate position:

$$\mathrm{logit}\left(S_{i,m}\right) = \beta_{0,m} + \beta_{1,m} Q_{i,m,d} + \beta_{2,m} I\left(\mathrm{DCC}_{i,m,d} = \mathrm{open}\right) + \varepsilon_{S,g,m}$$

where m indexes reaches 0, …, 8 (Figure 1), logit(·) is the logit link function, $\beta_{0,m}$ is the intercept, $\beta_{1,m}$ is the slope for the effect of discharge on survival, $\beta_{2,m}$ is the effect of Delta Cross Channel position on survival, $Q_{i,m,d}$ is the discharge of the Sacramento River at Freeport on day d that individual i entered reach m, $I\left(\mathrm{DCC}_{i,m,d} = \mathrm{open}\right)$ is an indicator function resolving to 1 if the DCC is open on day d that individual i entered reach m, and $\varepsilon_{S,g,m}$ is a normally distributed deviation for the gth release group in reach m with mean zero and standard deviation $\xi_{S,m}$.

Median travel time was expressed as a function of covariates in a similar manner as survival:

$$\mu_{i,m} = \alpha_{0,m} + \alpha_{1,m} Q_{i,m,d} + \alpha_{2,m} I\left(\mathrm{DCC}_{i,m,d} = \mathrm{open}\right) + \varepsilon_{\mu,g,m}$$

where $\mu_{i,m}$ is the mean of log-normal travel time distribution for the ith individual in the mth reach, exp($\mu_{i,m}$) is the median travel time, and $\alpha_{i,m}$ are slope and intercept coefficients.

In this model, survival is constant among individuals that enter a given reach on a particular day but varies among release groups according to the random effect term ε. Travel time influences survival only through its effect on arrival times to a given telemetry station, which determines the discharge that individuals experienced when they entered a given reach. The standard deviation of the random effects, ξ, estimates variation in mean travel time and survival among release groups over that explained by covariates. This term can be thought of as a measure of process error for unmeasured factors that vary among release groups migrating through a given reach (e.g., predator density). The DCC gate position is included as a covariate since the effect of opening the DCC gate is to reduce discharge in downstream reaches. Therefore, $\alpha_{2,m}$ and $\beta_{2,m}$ was set to zero for reaches located upstream of the of the Delta Cross Channel (i.e., for *m* = 0, ..., 3).

The Perry et al. (in prep.) analysis found a relationship between river inflows and median travel times in all reaches of the Delta (Figures 2 and 3). In contrast, their analysis found considerable variation in the flow-survival relationship among reaches (Figures 2 and 3). In the upper reaches of the Delta (Reaches 1 and 2; Figure 1), survival was consistently high regardless of inflows , whereas in the strongly tidal reaches (reaches 7 and 8) there was no significant relationship between river inflows and reach-specific survival despite a relationship between inflow and travel time. The strongest flow-survival relationships were identified in the three reaches that transition from river-driven to tidally-driven flows (Reaches 3, 4, and 5).

The product of reach-specific survival for a given migration pathway between Freeport (Site A_2 in Figure 1) and Chipps Island (Site A_6 in Figure 1) yields the probability of surviving through each migration route at a given river discharge. Route-specific survival for all routes increased with river discharge but approach an asymptote, leveling off at about 0.7 for the Sacramento River and Sutter and Steamboat Sloughs and about 0.35 for fish entering Georgiana Slough when river discharges increases beyond 30,000 – 40,000 ft^3/s (Figure 4). The reach-specific survival relationships indicate that the asymptote in route-specific survival was driven by the survival in the strongly tidal reaches (Reaches 7 and 8) since survival for all other reaches approached 1 as flow increased, but remained constant with flow for the strongly tidal reaches (Figure 3). Expected travel time distributions through each migration route decreased as river flow increased, with migration routes leading to the interior Delta (Georgiana Slough and the Delta Cross Channel) having longer travel times than other routes (Figure 5).

Migration Routing

To simulate overall survival through the Delta as a function of inflows requires a model for how river inflows affect the proportion of fish using each of the four primary migration routes through the Delta. Fish first enter Sutter and Steamboat Sloughs at its junction with the Sacramento River (Site B_1 and A_3 in Figure 1). Fish that remain in the Sacramento River may then enter the DCC (Site C_1) and Georgiana Slough (Site D_1) further downstream. For each migration route, we related daily proportions of fish entering each route to daily river discharge at Freeport.

For Sutter and Steamboat Slough, we analyzed acoustic telemetry on late-fall Chinook salmon from a study conducted in 2014 (DWR, in review). During this study, 3,418 acoustic tagged fish were detected at this river junction over a 58-day period. We conducted a logistic regression analysis that related the daily fraction of discharge entering Sutter and Steamboat Slough to the daily proportion of fish entering this route. Because fish were released daily at Sacramento, daily sample sizes averaged 58 fish (interquartile range = 43-83 fish), providing adequate sample sizes for the analysis. Daily river discharge varied from 9,146 – 28,051 ft^3/s over the 58-day period. Although initial analysis revealed a direct relation between discharge at Freeport and the probability of entering Sutter and Steamboat Slough, extending this relationship beyond the range of flow observed in the study suggested that entrainment increased in a linear fashion with flow. In contrast, the fraction of discharge entering Sutter and Steamboat increases at low flows owing to tidal forcing, but then stabilizes to a constant fraction as river inflow dampens tidal forcing. Thus, by using the ratio of Sutter and Steamboat discharge relative to Freeport discharge as a covariate, extending this relationship beyond the range of observed flows leads to an asymptotic relationship of entrainment with respect to discharge at Freeport (Figure 6). Although empirical data at higher flows is required to substantiate this relationship, we feel that this approach is consistent with the hypothesis that entrainment is related to the relative quantity of discharge entering this route rather than the absolute amount. The analysis suggests that the proportion of fish entering Sutter and Steamboat Slough increase from about 0.1 at 5,000 ft3/s to about 0.4 at 80,000 ft^3/s (Figure 6).

We summarize results of the multinomial model of Perry et al. (2015) to predict daily entrainment probabilities into Georgiana Slough and the Delta Cross Channel. This river junction experiences tidally reversing flows when inflows at Freeport are less than approximately 23,000 ft^3/s at Freeport. Perry et al. (2015) showed that entrainment into these migration routes depended on the tidal conditions when fish arrived at the river junction. Since the model predicts the probability of an individual entering each route as a function of the “instantaneous” river discharge (i.e., discharge measured at 15-minute intervals) at the time of fish arrival, we used this model to calculate entrainment probabilities based on 15-minute discharge records occurring during the time period the study was conducted (December through February of 2007 – 2009). We then related the mean daily entrainment probability to daily discharge at Freeport. Specifically, we used a segmented linear regression to relate the daily probability of entering Georgiana Slough with the DCC gate closed to Freeport discharge. For the DCC gate open, we used linear regression to relate the daily probability entering the DCC and Georgiana Slough to Freeport discharge. The segmented regression indicates that daily entrainment probabilities into Georgiana Slough initially decline with increasing discharge, but then change little as discharge increases above about 20,000 ft^3/s (Figure 7). Although the maximum discharge for this analysis was about 40,000, the expected entrainment into Georgiana Slough at 80,000 was 0.33 and is consistent with empirical evidence that showed entrainment into Georgiana Slough ranged from 0.244 to 0.299 at a Freeport discharge of 80,000 ft^3/s (Perry et al. 2014).

Simulating Survival under the PA and NAA Scenarios

To understand the effect of the North Delta Diversion on survival and travel time of juvenile late-fall Chinook salmon, we used the analysis of Perry et al (in prep.) to simulate travel time, survival, and migration routing using the CalSim model runs for the No Action Alternative (NAA) and Proposed Action (PA). The simulation produces a Delta-wide (Freeport to Chipps Island) survival probability and travel time distributions for a cohort of fish entering the Delta at Freeport on each day of the 82 year daily time series of Delta inflows. For each day of the 82 year time series, travel time and survival was simulated as follows:

1) Initiate the simulation with 10,000 fish at Freeport on day *t*.
2) Calculate survival in Reach 1 given Freeport discharge on day *t*. Survival was calculated based on the median of the posterior distributions of the parameters relating survival to inflows at Freeport.
3) Draw individual travel times through Reach 1 from a log-normal distribution where the mean of the distribution depends on the river flow on day *t*. This yields a distribution of arrival times at the junction of Sutter and Steamboat Slough with the Sacramento River.
4) Draw the route taken by each fish from a Bernoulli distribution where the probability of entering Sutter and Steamboat Slough is a function of Bypass discharge on the day each fish arrives at the junction.

5) Calculate the survival probability of each individual for the next reach downstream (Sacramento River or Sutter and Steamboat Sloughs) given the river flow on day each fish entered the reach.
6) Draw travel times for each individual for the next downstream reach given the flows on the day each fish entered the reach.
7) For fish remaining in the Sacramento River, draw the route taken by fish at the junction of the Sacramento River with the Delta Cross Channel (DCC) and Georgiana Slough from a multiple Bernoulli distribution where the probability of entering each route depends on the position of the DCC gates and Freeport flows on the day each fish arrived at the junction.
8) Repeat steps 5 and 6 for all remaining reaches.

Thus, the simulation yields reach-specific expected survival probabilities, reach-specific travel times, and routing histories for a cohort of 10,000 individuals entering the Delta at Freeport on each day of the 82-year time series of CalSim output. By using this approach, our simulation emulates the effect of daily flow variation on through-Delta survival and travel time for a cohort of fish that enter the Delta on a given day. For example, although two cohorts may enter the Delta under identical flows at Freeport, survival and travel time of these cohorts would differ if one cohort entered under an ascending hydrograph and one entered during a descending hydrograph.

The simulation output for each day was then summarized to provide a number of useful statistics for each daily cohort:

- The proportion of fish using each unique migration route.
- The mean survival for each unique migration route, calculated by first taking the product of reach-specific survival between Freeport and Chipps Island for each individual and then taking the mean survival over all individuals.
- Overall survival through the Delta, calculated as the mean survival over all individuals. Since routing for each individual was a randomly drawn at each river junction, the mean survival is implicitly weighted by the proportion of fish that used each route.
- Median travel time by route and over all routes. Median travel time was calculate by first summing reach-specific travel times for each individual between Freeport and Chipps

Island and then taking the mean of the logarithm of travel times (by route and over all routes).

- Daily difference in survival and median travel time between PA and NAA scenarios.

We summarize the difference in daily through-Delta survival between PA and NAA with boxplots that display the distribution of survival differences among years for a given date or for given months. To understand how these differences arise, it is useful to examine how the individual components of migration routing, survival, and travel time contribute to overall survival in a particular year. In Figures 8-13, we illustrate detailed model output for 1943, a wet water year that exhibited bypass flows (flow remaining in the Sacramento River below the North Delta Diversion) ranging from <5,000 ft^3/s to > 50,000 ft^3/s.

References

California Department of Water Resources (DWR). In review. 2014 Georgiana Slough Floating Fish Guidance Structure Performance Evaluation Project Report.

King, R., B. Morgan, O. Gimenez, and S. Brooks. 2009. Bayesian analysis for population ecology. CRC Press.

Michel, C.J., A.J. Ammann, S.T. Lindley, P.T. Sandstrom, E.D. Chapman, M.J. Thomas, G.P. Singer, A.P. Klimley, and R.B. MacFarlane. 2015. Chinook salmon outmigration survival in wet and dry years in California's Sacramento River. Canadian Journal of Fisheries and Aquatic Sciences 72: 1749-1759.

Perry, R.W., A.C. Pope, J.G. Romine, P.L. Brandes, J.R. Burau, A. Blake, A. Amman, and C. Michel. In preparation. Flow-mediated effects on travel time and survival vary among reaches in the Sacramento-San Joaquin River Delta. To be submitted to the Canadian Journal of Fisheries and Aquatic Sciences.

Perry R.W., J.R. Skalski, P.L. Brandes, P.T. Sandstrom, A.P. Klimley, A. Ammann, and R.B. MacFarlane. 2010. Estimating survival and migration route probabilities of juvenile Chinook salmon in the Sacramento–San Joaquin River Delta. North American Journal of Fisheries Management 30:142-156.

Perry R.W., P.L. Brandes, J.R. Burau, A.P. Klimley, B. MacFarlane, C. Michel, and J.R. Skalski. 2013. Sensitivity of survival to migration routes used by juvenile Chinook salmon to negotiate the Sacramento-San Joaquin River Delta. Environmental Biology of Fishes 96:381-392.

Perry R.W., J.G. Romine, N.S. Adams, A.R. Blake, J.R. Burau, S.V. Johnston, and T.L Liedtke. 2014. Using a non-physical behavioral barrier to alter migration routing of juvenile Chinook salmon in the Sacramento-San Joaquin River Delta. River Research and Applications 30: 192-203.

Perry R.W., P.L. Brandes, J.R. Burau, P.T. Sandstrom, and J.R. Skalski. 2015. Effect of tides, river flow, and gate operations on entrainment of juvenile salmon into the interior Sacramento–San Joaquin River Delta. Transactions of the American Fisheries Society 144: 445-455.

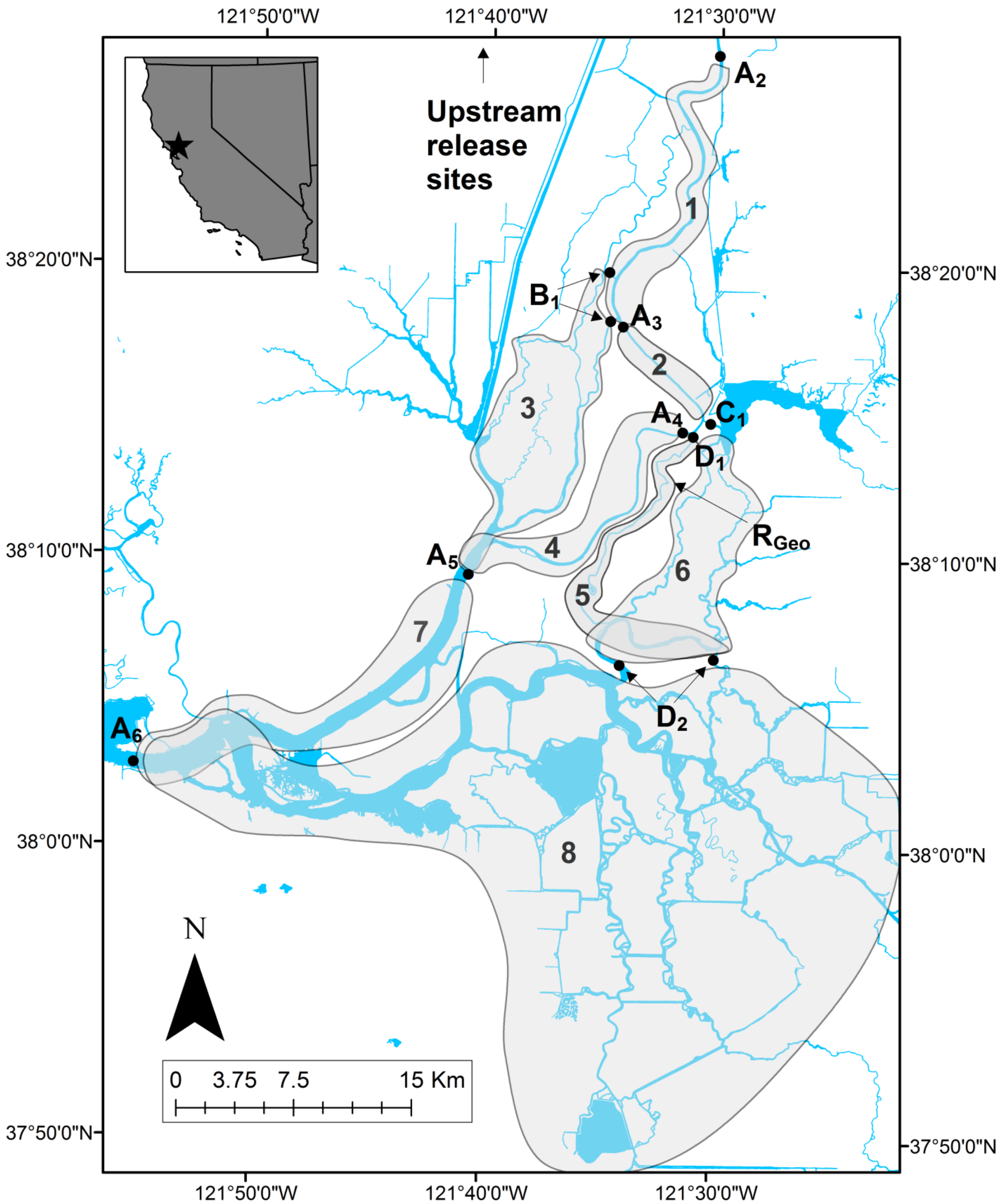

Figure 1. Map of the Delta with dots showing location of telemetry stations and shaded regions highlighting the eight reaches in which reach-specific survival and travel times were estimated. Telemetry stations are coded by the *i*th telemetry station in the *h*th route (A = Sacramento River, B = Sutter and Steamboat Slough, C = Delta Cross Channel, D = Georgiana Slough). Reach 0 from Sacramento to Freeport (A_2) was considered an "acclimation" reach to allow fish to resume nominal migration behavior after release. RGeo indicates a release site in Georgiana Slough to increase the sample size of fish migrating through the interior Delta (Reach 8).

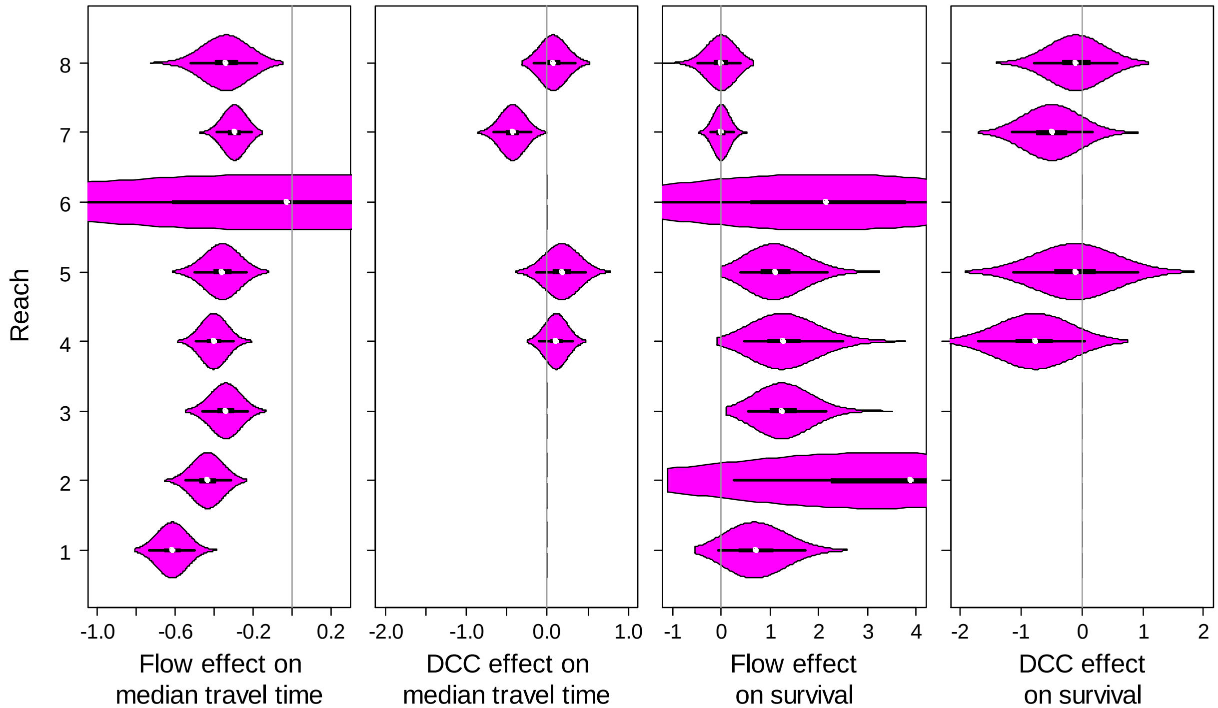

Figure 2. Violin plots showing the posterior distributions of slope parameters for the effect of Sacramento River discharge at Freeport on survival and median travel time. The white dot shows the median, the heavy bar displays the interquartile range, and the thin bar shows the 2.5th to 97.5th percentile of the posterior distribution.

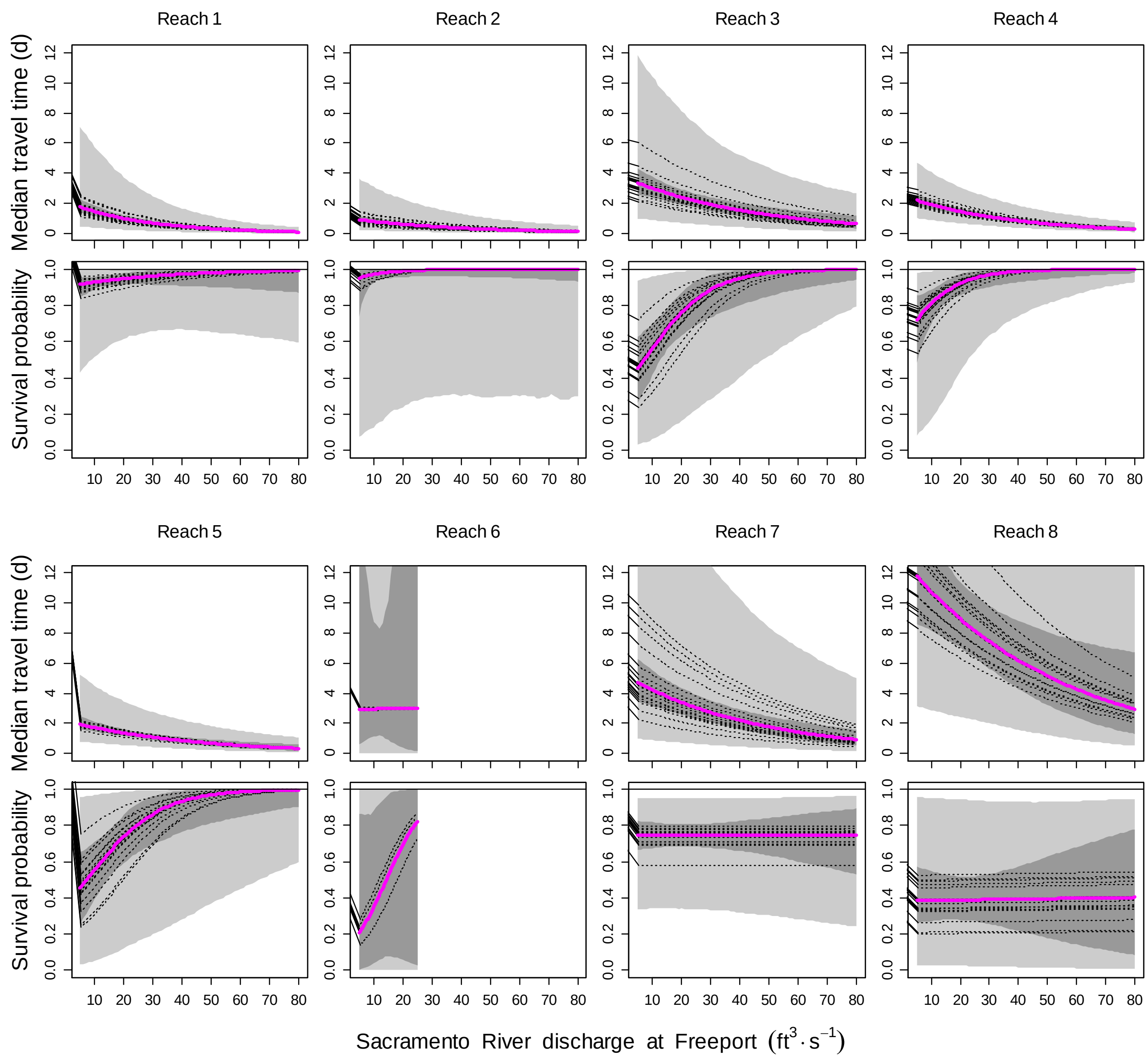

Figure 3. Reach-specific relationships of survival and travel time with Sacramento River discharge at Freeport (ft^3/s x 1000). The heavy magenta line shows the relationship plotted at the median of the posterior distribution of the parameters. The thin dotted lines show variation in the relationship among 17 release groups. The dark gray region shows 95% credible intervals about the median relationship. The light gray region shows 95% credible intervals including both parameter uncertainty and uncertainty in the estimate of the variation among release groups.

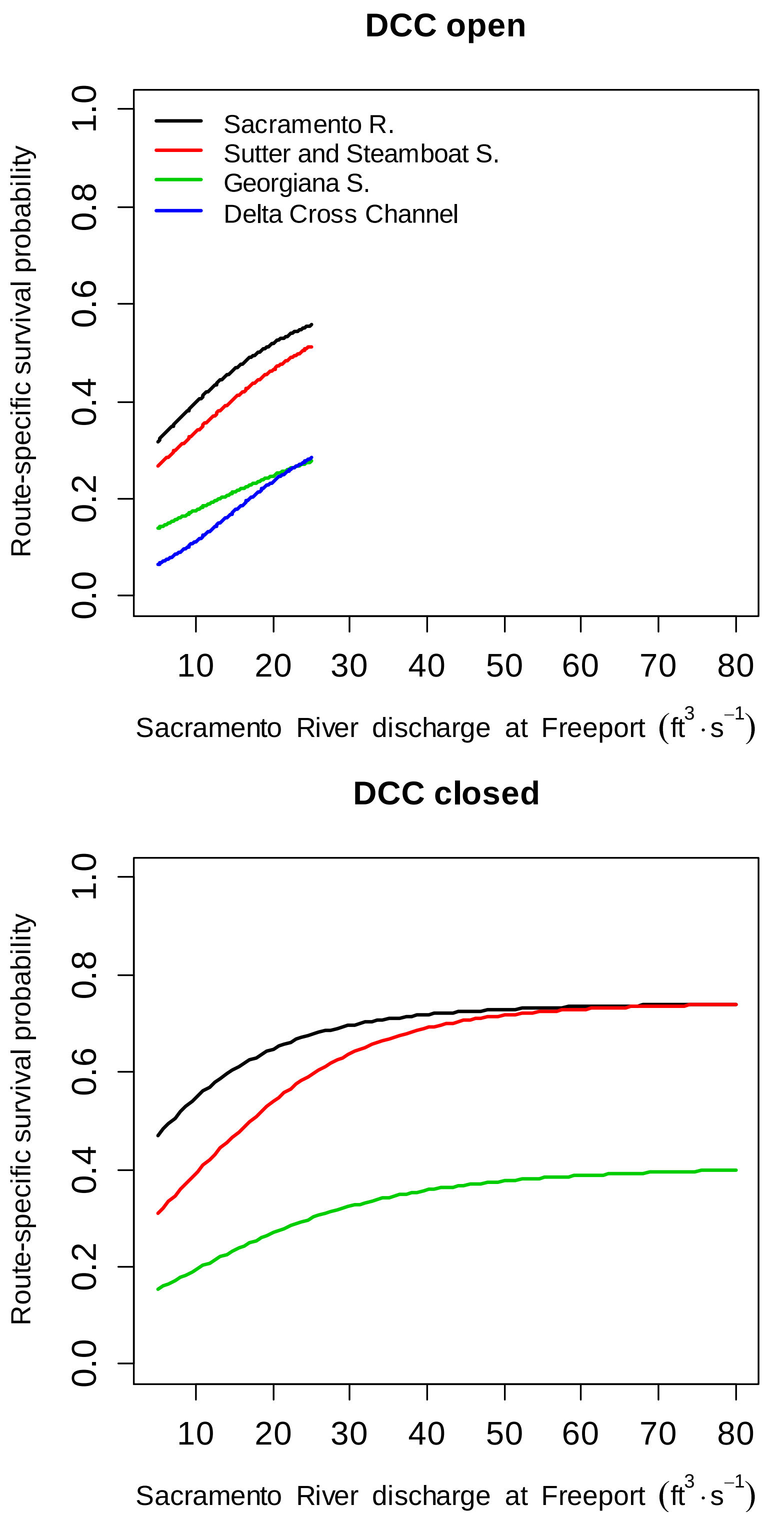

Figure 4. Route-specific survival between Freeport and Chipps Island as a function of Sacramento River discharge at Freeport. Route-specific survival was calculated as the product of reach-specific survival based on the posterior medians of the parameters.

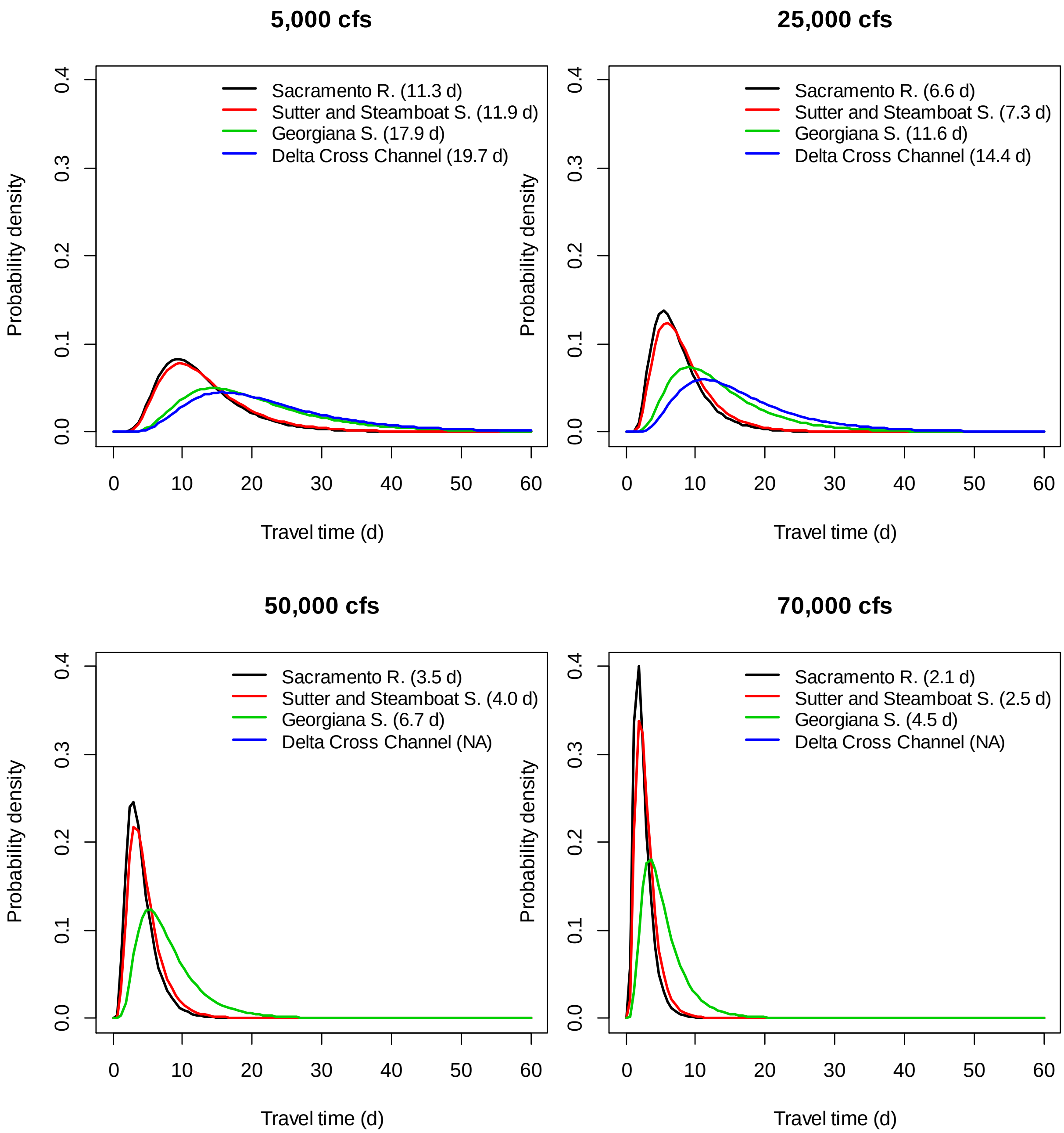

Figure 5. Route-specific travel time distributions between Freeport and Chipps Island for a range of Sacramento River discharge at Freeport. The median travel times for each route is given in the legend. Travel time distributions were based on posterior medians of parameters for reach-specific travel time distributions. Distributions are shown assuming closed Delta Cross Channel gates.

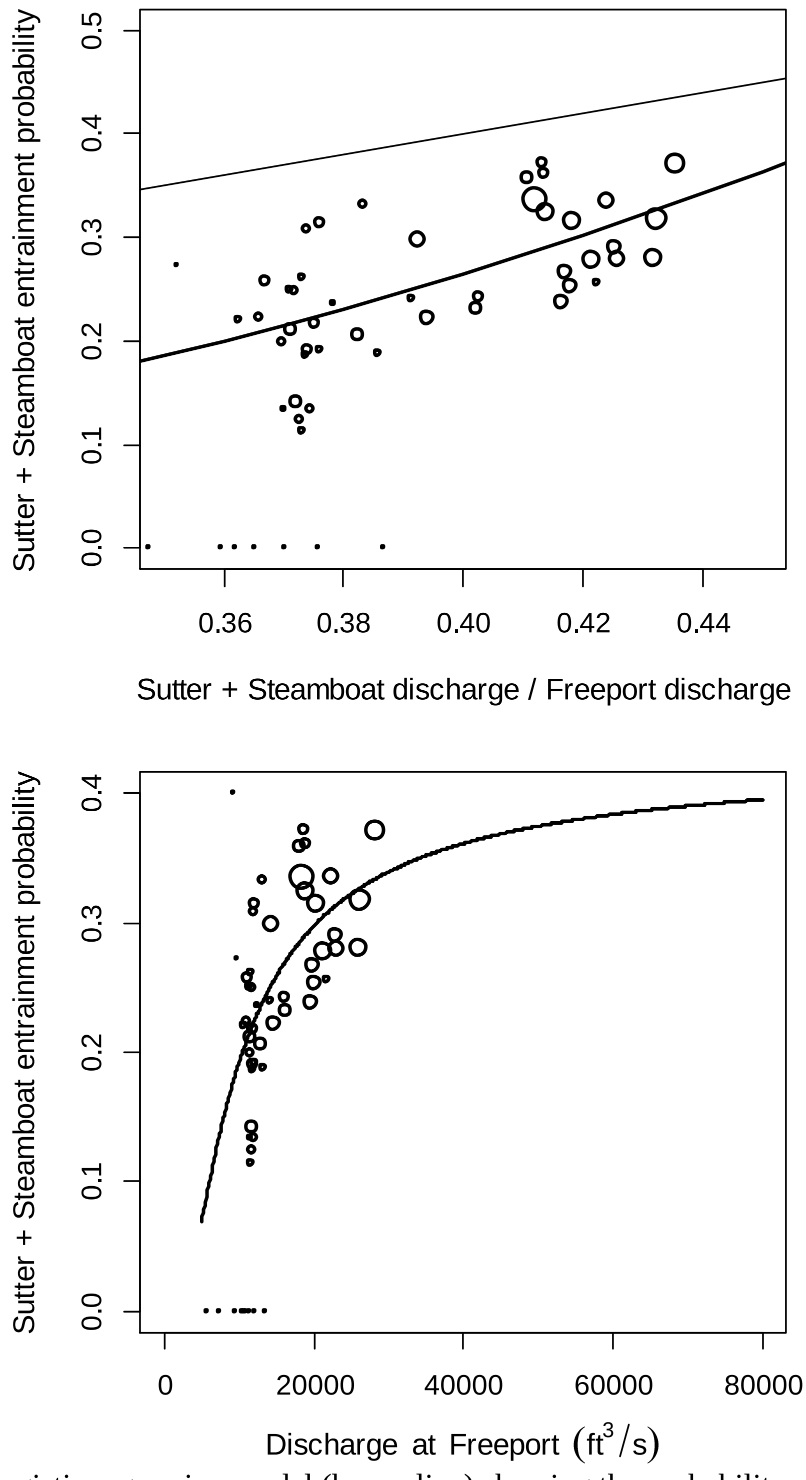

Figure 6. Logistic regression model (heavy line) showing the probability of entering Sutter and Steamboat Slough as a function of the ratio of Sutter + Steamboat discharge to Freeport discharge (top panel) and discharge of the Sacramento River at Freeport (bottom panel). In the top panel, the thin line shows where the proportion of fish entering Sutter and Steamboat sloughs is equal to the proportion of flow enter the sloughs. Data were obtained from acoustically tagged late-fall Chinook salmon collected in 2014 during the Georgiana Slough non-physical barrier study. The size of the symbols are scaled proportionately to the daily sample size of fish passing the river junction each day.

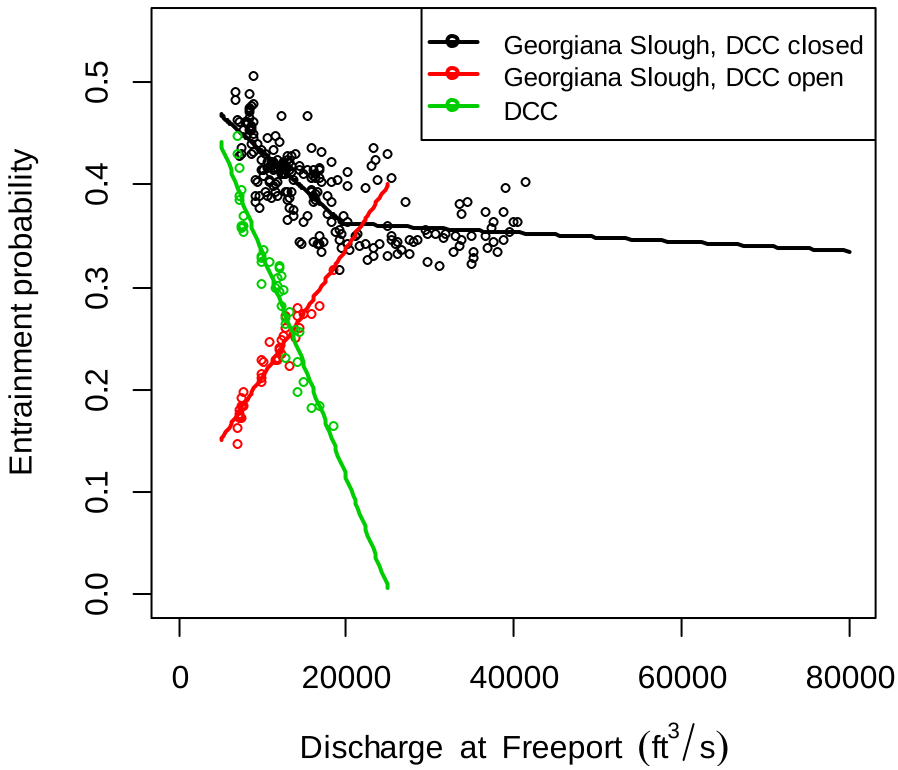

Figure 7. Daily entrainment probability into Georgiana Slough and the Delta Cross Channel as a function of discharge of the Sacramento River at Freeport. Daily routing probabilities were estimated by fitting linear models to daily entrainment probabilities that were calculated using the entrainment model of Perry et al. (2015).

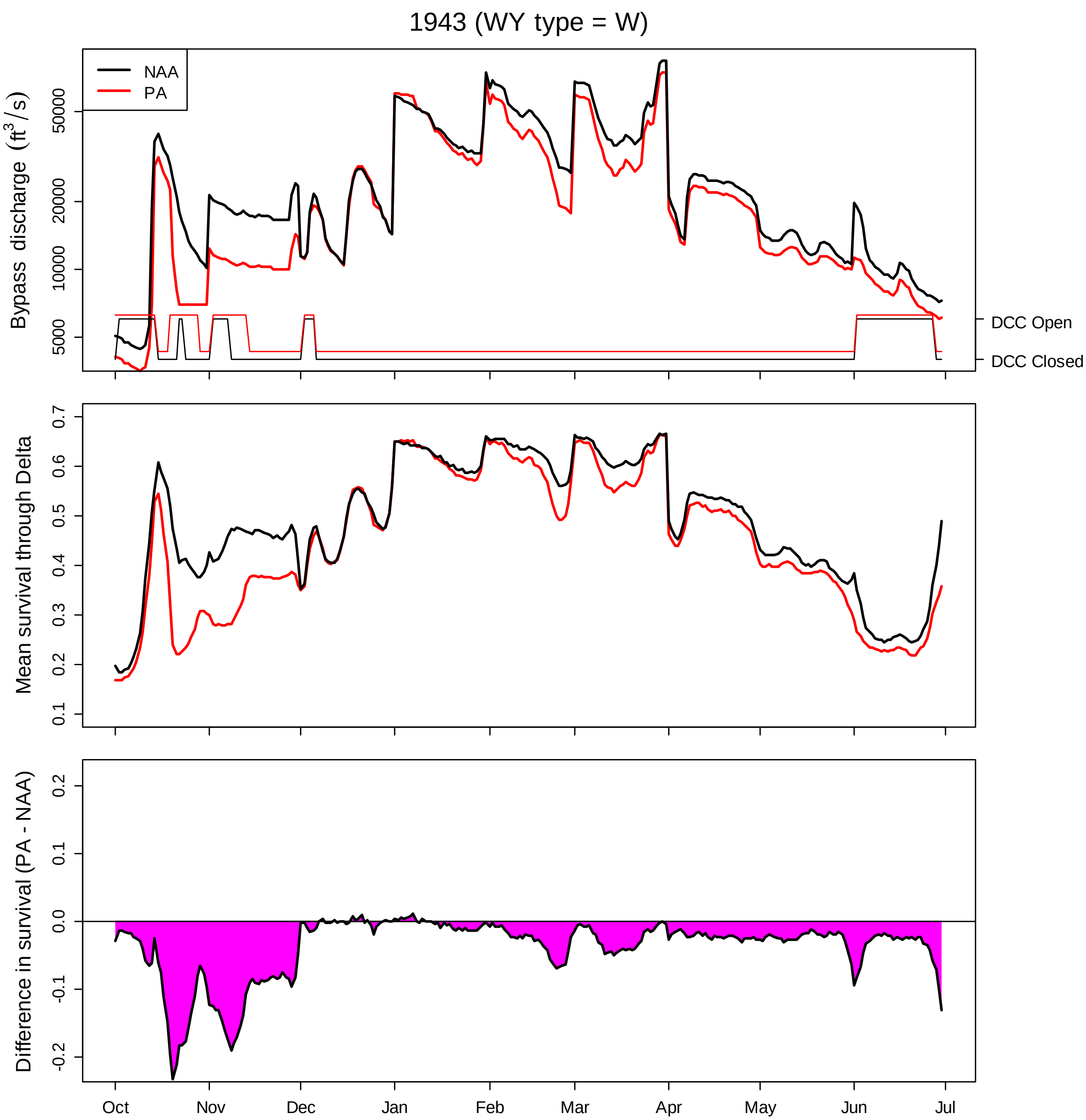

Figure 8. Mean daily survival through the Delta simulated for the Proposed Action (PA) and No Action Alternative (NAA, middle panel). Heavy lines in the top panel shows bypass discharge and thin lines show DCC operation of open or closed on the second *y*-axis. The bottom panel shows the difference in daily survival between scenarios. Discharge in the top panel is shown on a logarithmic scale to highlight variation in discharge when discharge is low.

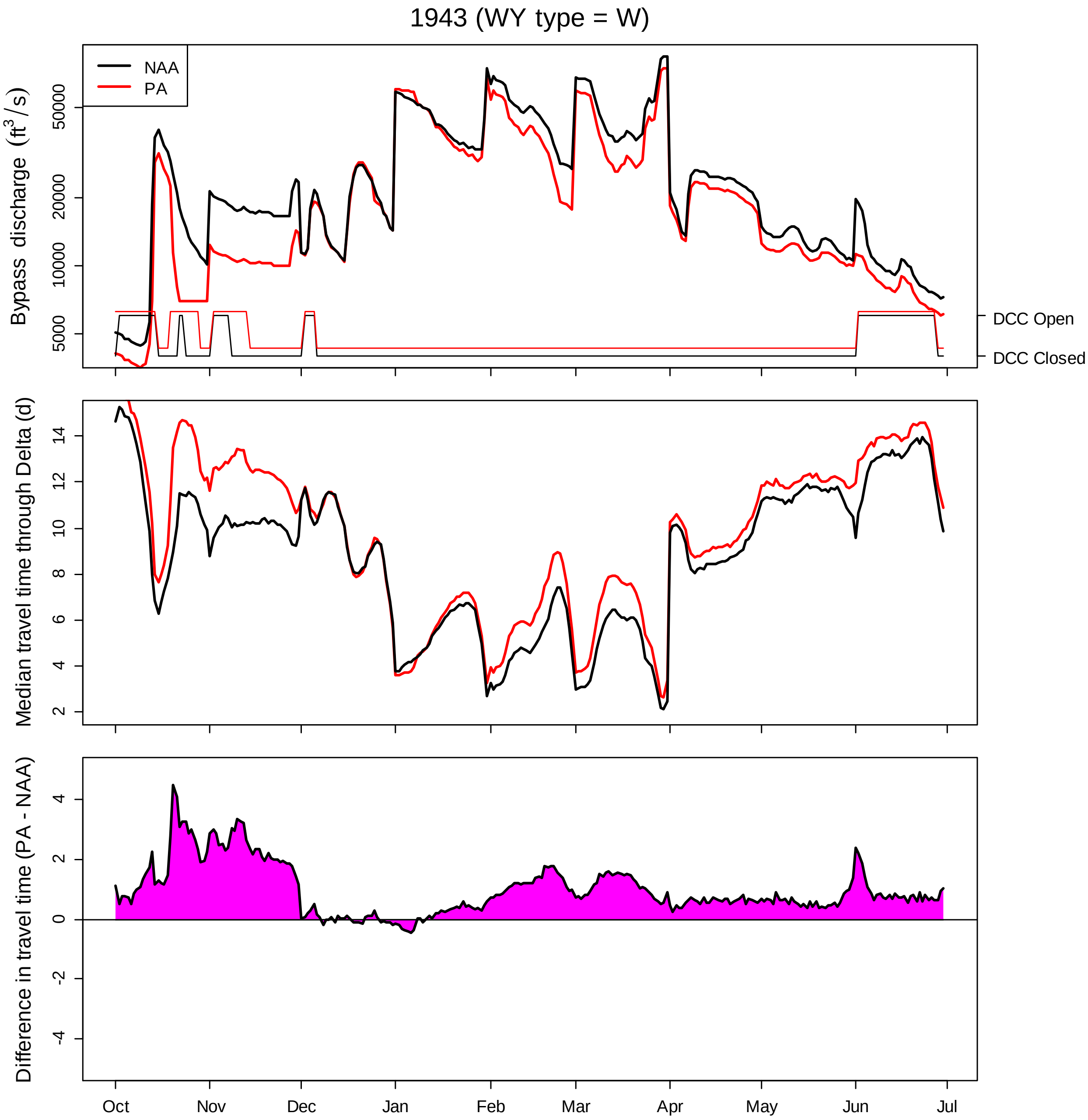

Figure 9. Median daily travel time through the Delta simulated for the Proposed Action (PA) and No Action Alternative (NAA, middle panel). Heavy lines in the top panel shows bypass discharge and thin lines show DCC operation of open or closed on the second *y*-axis. The bottom panel shows the difference in median travel time between scenarios. Discharge in the top panel is shown on a logarithmic scale to highlight variation in discharge when discharge is low.

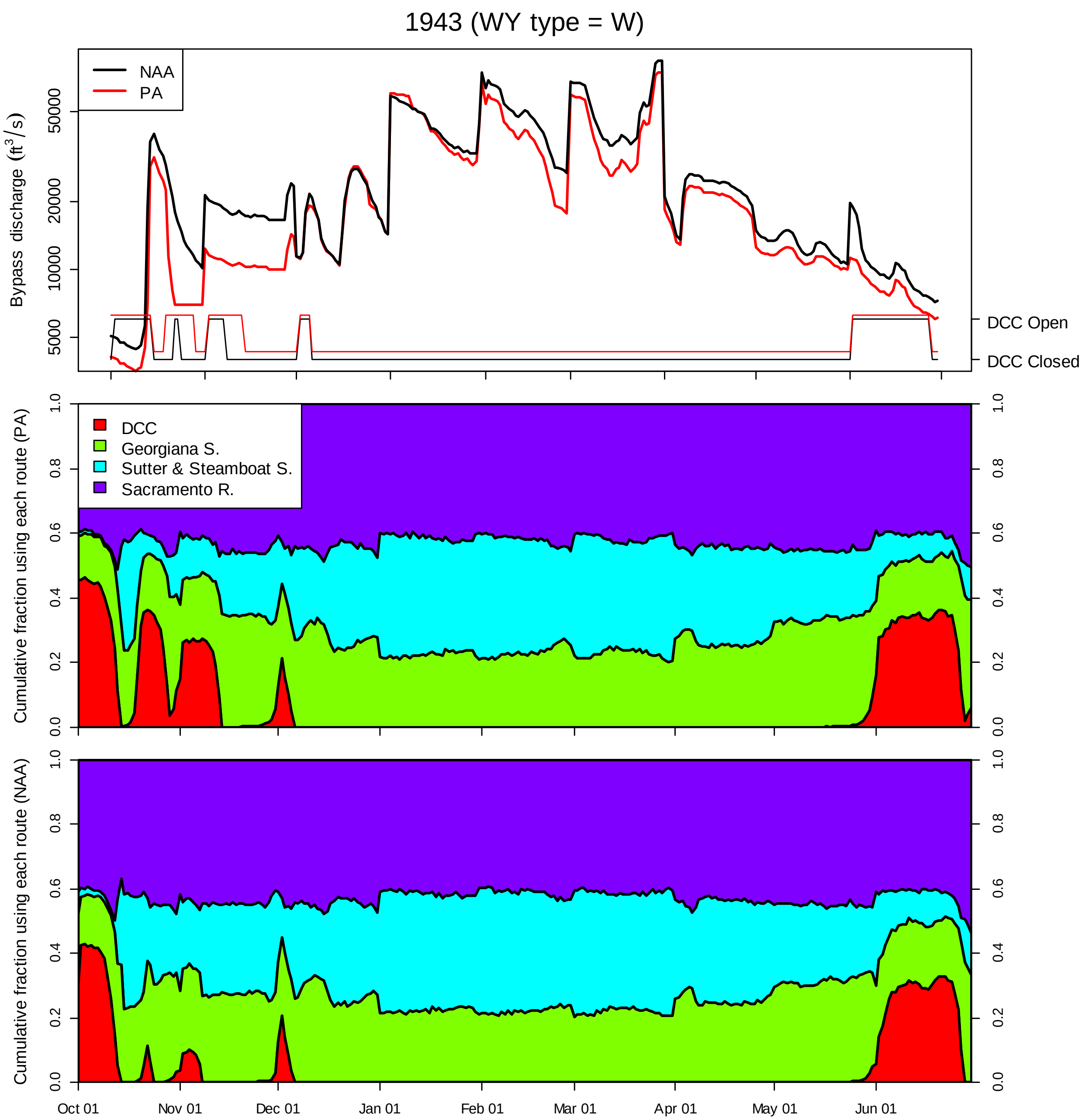

Figure 10. Stacked line plots showing the daily cumulative migration route probabilities for the Proposed Action (PA, middle panel) and No Action Alternative (NAA, bottom panel). Heavy lines in the top panel shows bypass discharge and thin lines show DCC operation of open or closed on the second *y*-axis. The bottom panel shows the difference in median travel time between scenarios. Discharge in the top panel is shown on a logarithmic scale to highlight variation in discharge when discharge is low.

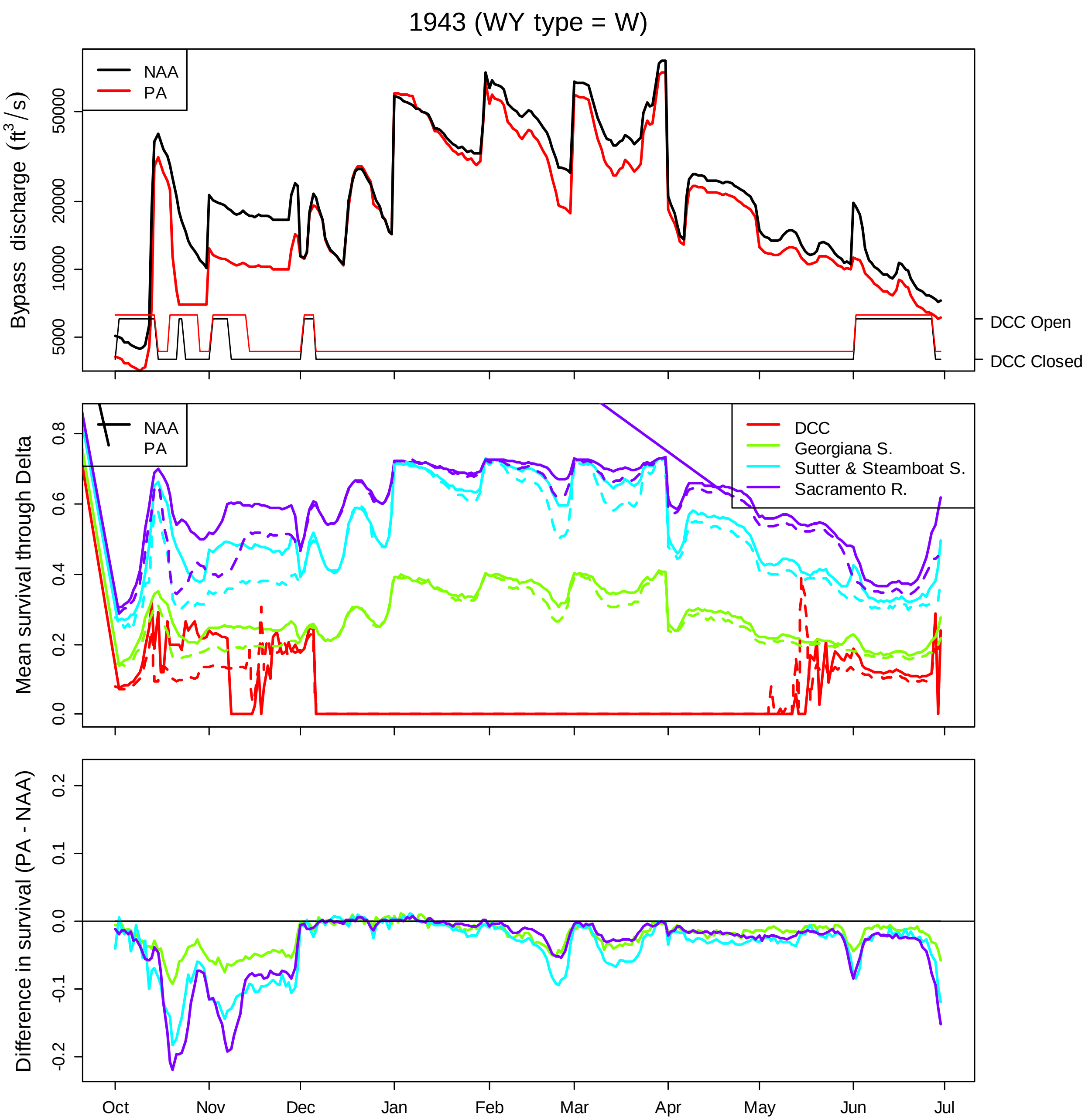

Figure 11. Mean daily route-specific survival through the Delta simulated for the Proposed Action (PA) and No Action Alternative (NAA, middle panel). Heavy lines in the top panel shows bypass discharge and thin lines show DCC operation of open or closed on the second *y*-axis. The bottom panel shows the difference in daily route-specific survival between scenarios. Differences in Delta Cross Channel survival is not shown owing to difference in daily operations of the DCC between scenarios. Discharge in the top panel is shown on a logarithmic scale to highlight variation in discharge when discharge is low.

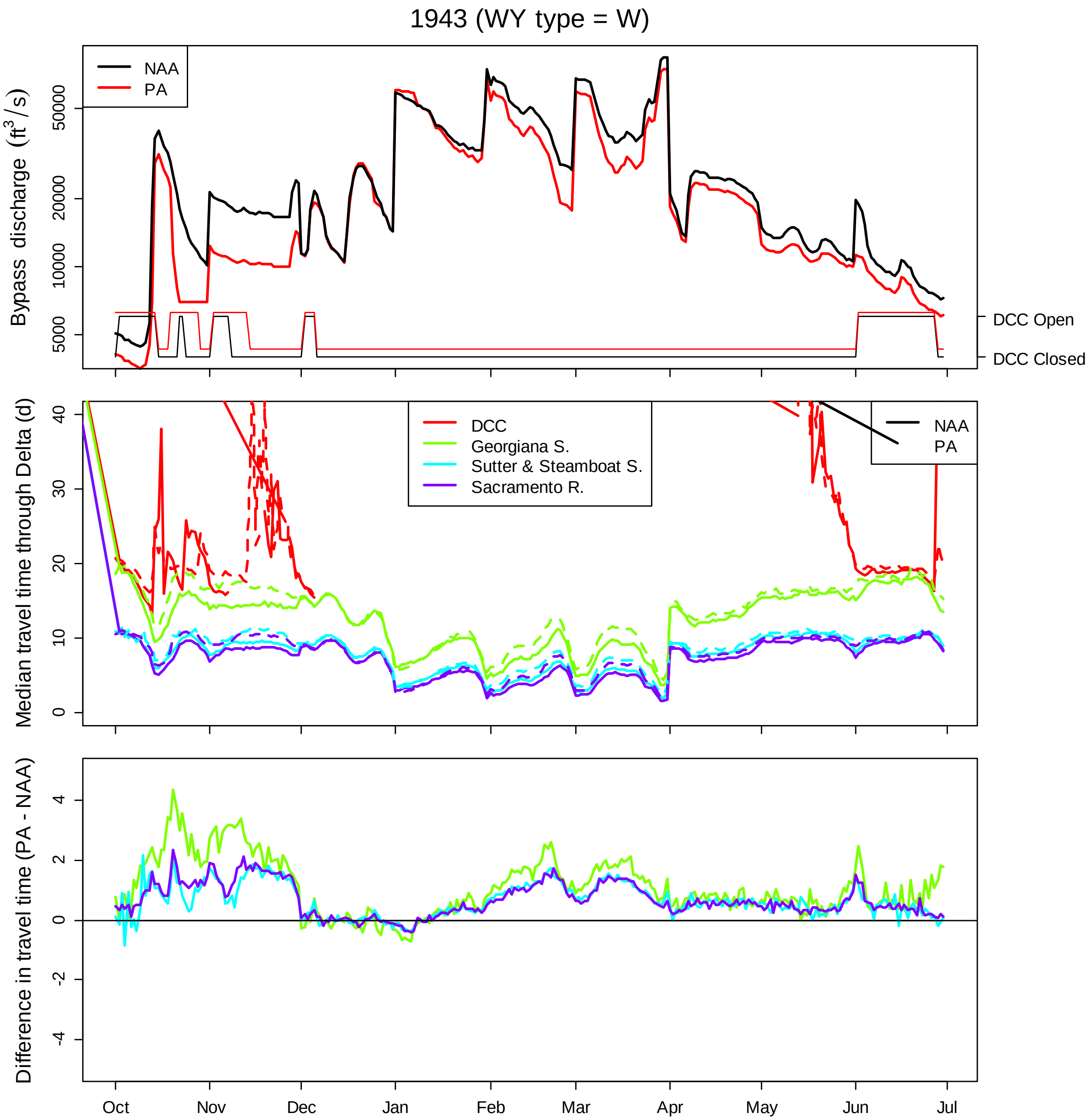

Figure 12. Median daily route-specific travel time through the Delta simulated for the Proposed Action (PA) and No Action Alternative (NAA, middle panel). Heavy lines in the top panel shows bypass discharge and thin lines show DCC operation of open or closed on the second *y*-axis. The bottom panel shows the difference in daily route-specific travel time between scenarios. Differences in Delta Cross Channel survival is not shown owing to difference in daily operations of the DCC between scenarios. Discharge in the top panel is shown on a logarithmic scale to highlight variation in discharge when discharge is low.

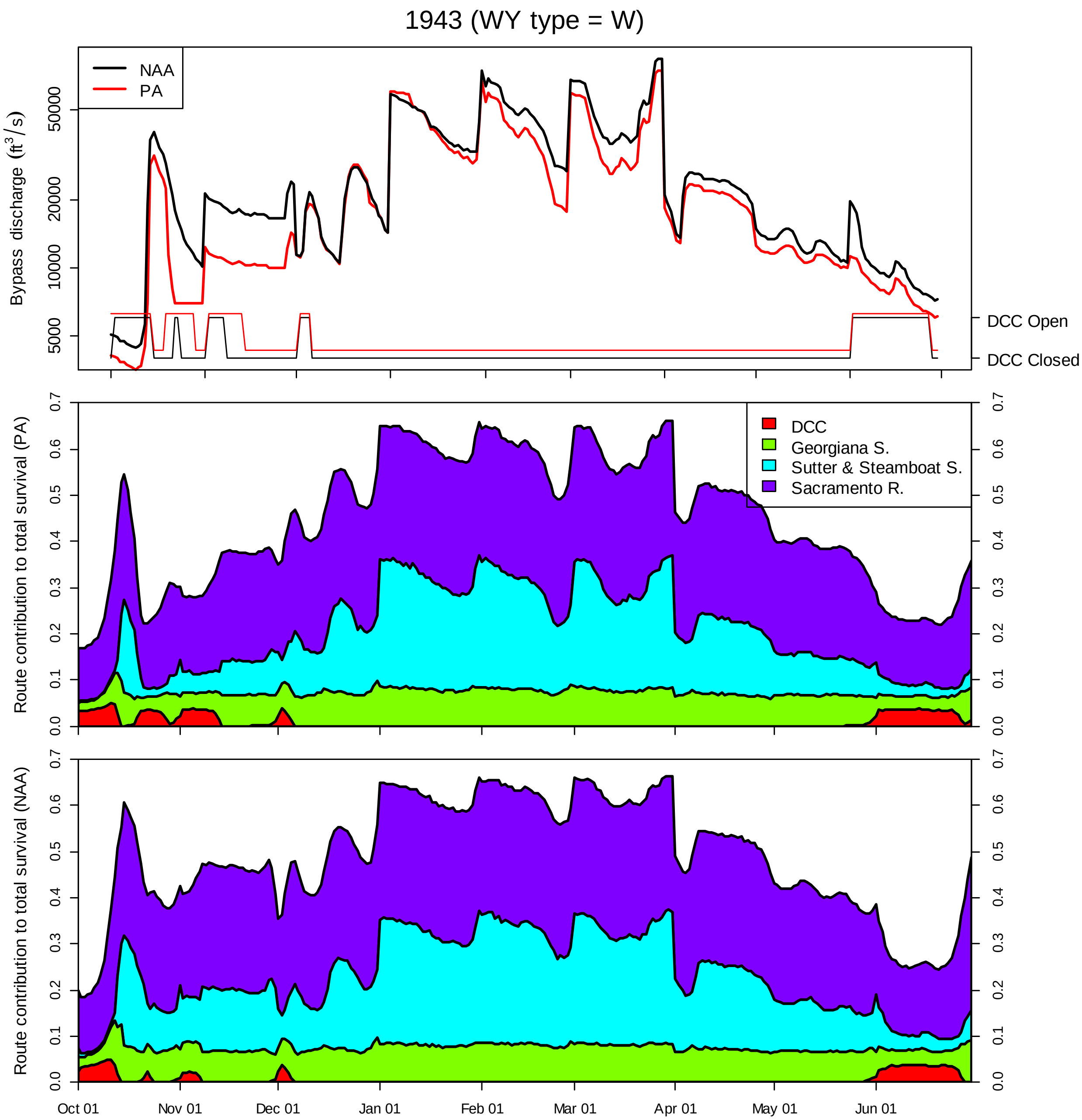

Figure 13. Stacked line plot showing each route's contribution to total survival simulated for the Proposed Action (PA, middle panel) and NAA (No Action Alternative, bottom panel). The width of each bar is the product of the probability of surviving a given migration route and the probability of migrating through that route such that the top line is the total survival through the Delta. Heavy lines in the top panel shows bypass discharge and thin lines show DCC operation of open or closed on the second *y*-axis. Discharge in the top panel is shown on a logarithmic scale to highlight variation in discharge when discharge is low.